THE MÖSSBAUER EFFECT IN SUPPORTED MICROCRYSTALLITES

FRANK J. BERRY

University of Cambridge Chemical Laboratory, Cambridge, England

I. Introduction 255
II. Iron and Iron Oxides 259
A. Iron Oxides 259
B. Hydrogen Reduction of Iron Oxides 269
C. Heating of Iron Oxides *in Vacuo* 272
D. Catalysts and the Adsorption of Gases 276
III. Tin 280
IV. Gold, Europium, and Ruthenium 281
References 282

I. Introduction

In 1958, Rudolph Mössbauer (*1*) discovered that γ-ray emission without loss of energy from recoil of the nucleus could be achieved by incorporating the emitting nucleus in a crystal lattice. The phenomenon is known as the "Mössbauer effect."

Mössbauer also demonstrated the inverse process of recoil-free absorption of γ-rays over a narrowly defined energy spectrum when the absorbing nucleus is similarly bound in a crystal lattice. This resonance process occurs only when the nuclear energy levels of both absorber and emitter are identical. When the absorber nucleus is in a different electronic environment from the source nucleus, the nuclear energy levels no longer coincide and absorption can only occur when the energy of the photons emitted by the source is modified using the Doppler effect. This modification is produced by oscillating the absorber relative to the emitter, or vice versa, and a range of velocities are scanned until maximum absorption occurs. A Mössbauer spectrum usually consists of a plot of γ-ray counts against the relative velocity in millimeters per second of the source with respect to the absorber (Fig. 1). The magnitude of the required applied velocity is known as the chemical isomer shift, δ, of the absorber relative to the source employed. It is a measure of the difference in nuclear excitation energies between the nuclei in the source and the absorber that results

ISBN 0-12-023621-4

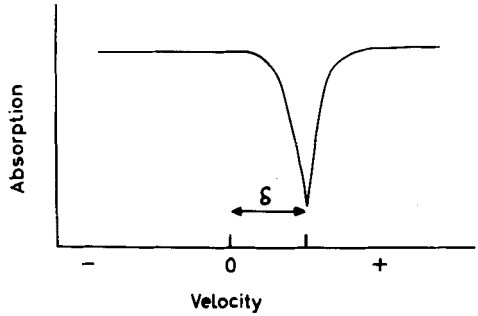

FIG. 1. Mössbauer spectrum showing the chemical isomer shift.

from their different electronic environments. Isomer shifts arise because the nucleus occupies a finite volume and during a nuclear gamma transition it is usual for the effective nuclear size to alter, thereby changing the nucleus–electronic field interaction energy. The nuclear excitation energy is sensitive to changes in the electron density at the nucleus, and the chemical isomer shift, which is an indication of the variation of this electron density in different compounds, is a function of the s-electron density at the nucleus. By making certain assumptions, it can be shown that the chemical isomer shift is given by

$$\delta = \text{constant} \times \frac{\Delta R}{R}\left(\left|\psi s(0)\right|_a^2 - \left|\psi s(0)\right|_s^2\right) \tag{1}$$

where $\Delta R/R$ is the fractional change in the nuclear charge radius on excitation and $\left|\psi s(0)\right|_a^2$ and $\left|\psi s(0)\right|_s^2$ are, respectively, the total s-electron densities at the nuclei of the absorber and source. In compounds containing iron-57, higher s-electron density results in a decreased, i.e. more negative, chemical isomer shift. The chemical isomer shift is, however, also sensitive to the d-electron density since the 3d electrons have a finite probability of penetrating the s-electron shell and thereby shielding s-electrons from the nucleus. The removal of d electrons, therefore, effectively increases the s-electron density at the nucleus and consequently ferric species have lower, i.e. more negative, chemical isomer shifts than ferrous species. Additionally, for iron atoms with the same oxidation state and electronic configuration and with identical ligands, the chemical isomer shift is dependent on the number and symmetry of the coordinating ligands (*2*, *3*). For this

reason tetrahedral iron compounds have a lower chemical isomer shift than octahedral compounds with the same ligands. It has also been suggested that the chemical isomer shift is affected in a small way by changes in ligands a number of atoms away from the iron atom (*4–6*).

Any nuclear state with a spin $I > \frac{1}{2}$ has a nuclear quadrupole moment, i.e., the nuclear charge distribution may be elongated along the intrinsic axis of symmetry labeled the z-axis in which case the nuclear quadrupole moment, Q, is positive or it may be compressed along this axis in which case Q is negative. The interaction of the nuclear charge density with asymmetric extranuclear electric fields, i.e., situations in which the principal components of the electric field gradient are such that $V_{zz} \neq V_{xx} \neq V_{yy}$, results in a splitting of the nuclear energy levels. The axes are labeled so that $V_{zz} > V_{xx} \geq V_{yy}$ and the electric field gradient may, therefore, be expressed in terms of V_{zz}, usually written as eq and an asymmetry parameter η which is described as:

$$\eta = \frac{V_{xx} - V_{yy}}{V_{zz}} \tag{2}$$

For the iron-57 isotope, the electric field gradient arises from (*a*) the charge distribution of the 3d electrons and (*b*) the charge distribution or crystal field of the neighboring ions in a crystal structure. The first term usually dominates the second. The coupling of Q to eq splits the excited $I = \frac{3}{2}$ level into two, whereas the $I = \frac{1}{2}$ ground level remains degenerate. Transitions from the ground state to these two excited levels can be observed as a two-peak spectrum as shown in Fig. 2 which is a reflection of the distortion of the crystal structure. The centroid of the two peaks relative to the source is equivalent to the chemical isomer shift, and the velocity difference between the two peaks in millimeters per second is called the quadrupole splitting, Δ, and is related to the quadrupole coupling by

$$\Delta = \tfrac{1}{2}e^2qQ\left(1 + \frac{\eta^2}{3}\right)^{1/2} \tag{3}$$

High-spin ferric compounds, which possess the iron nucleus in a spherically symmetric electronic configuration, usually have small quadrupole splittings (0–1 mm sec^{-1}), whereas high-spin ferrous species frequently have large quadrupole splittings arising from the sixth d electron. The quadrupole splitting has been found to be sensitive to changes in ligands a number of atoms away from iron (*5, 6*).

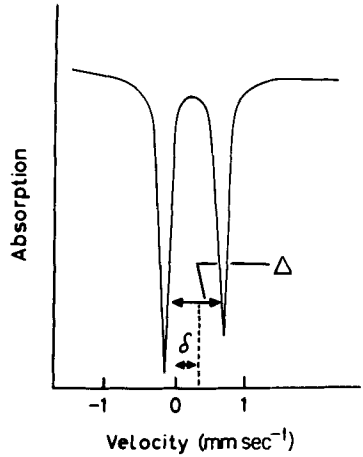

FIG. 2. Mössbauer spectrum showing quadrupole splitting (Δ).

If the nuclear dipole moment interacts with a magnetic field, all the degeneracy of the magnetic sublevels is lifted and each spin state splits into $2I + 1$ levels, where I is the nuclear spin quantum number. The Mössbauer spectrum of metallic iron, therefore, gives a six-peak pattern of equal spacing as a result of the magnetic field generated by ferromagnetic exchange interaction (Fig. 3). The spectrum is complicated by any contribution of quadrupole splitting to the magnetic splitting as in antiferromagnetic α-Fe_2O_3, which has an axially symmetric electric field gradient. In such a situation the shift in each of the levels of the excited state is $\epsilon = \frac{1}{4}e^2qQ$. The difference between the spacings of the pairs of outer peaks gives the quadrupole coupling constant. The magnetic field can also arise in paramagnetic

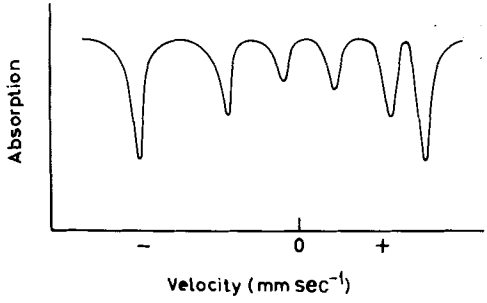

FIG. 3. Mössbauer spectrum showing magnetic hyperfine splitting.

species with long spin- lattice or spin-spin relaxation times that are temperature- and concentration-dependent, respectively.

Surface chemistry and catalytic activity are frequently dependent on surface area or crystallite size, and a knowledge of the electronic environment of surface nuclei is important in understanding the nature of catalysts and reactions at solid surfaces. Mössbauer spectroscopy, which examines directly the electronic environment at the nucleus, is a particularly favorable technique for the investigation of such matters, and several short discussions of the preliminary studies have now appeared (*7–15*). The examination of microcrystallites adsorbed onto high-area inert supports has been found to be informative in such investigations. The support disperses and maintains thin layers of microcrystallites over its high surface area and prevents sintering of the deposit during oxidation, reduction, and outgassing treatments.

The usual preparation of supported micrycrystalline samples by the incipient wetness technique involves the impregnation of a support, e.g., silica gel or alumina, with a solution of a metal salt to form a thick slurry that is subsequently dried and sometimes heat-treated.

II. Iron and Iron Oxides

A. Iron Oxides

Microcrystallites of iron oxides have been supported on silica gel and alumina by the incipient wetness technique and examined by Mössbauer spectroscopy. Bulk α-Fe_2O_3 has a corundum (α-Al_2O_3) crystal structure that involves a close-packed oxygen lattice containing ferric ions in octahedral sites. Above the Morin transition temperature (T_M = 263 K), bulk α-Fe_2O_3 shows a weak ferromagnetism due to the spins aligning with one of the vertical planes of symmetry making a small angle with the basal plane. Below T_M the spins are aligned along the [0001] axis and the oxide is pure antiferromagnetic. The magnetic ordering is reflected in the six-line Mössbauer spectrum of α-Fe_2O_3 which shows (*16*) the material to have a chemical isomer shift, δ (relative to iron) of 0.38 mm sec^{-1} and a quadrupole splitting of 0.12 mm sec^{-1}. The first Mössbauer investigation of microcrystalline Fe_2O_3 supported on alumina by Flinn *et al.* showed (*17*) a large quadruple split absorption, Δ 1.06 mm sec^{-1}, at 300 K, which remained constant at 77 K. The spectrum was interpreted in terms of the occupation by ferric ions of asymmetric octahedral environments on the surface of the alumina support that had one oxygen nearest neighbor missing. An expected quadrupole splitting, based on data pertaining

to such a model, of ca. 1.6 mm sec^{-1} was calculated. A chemical isomer shift, corrected (as are all chemical isomer shift data reported in this work) relative to natural iron of 0.30 mm sec^{-1} was reported. The different intensities of the two peaks that disappeared at 77 K were attributed to the Goldanskii–Karyagin effect which has its origins in the anisotropy of the recoil-free fraction parallel and normal to the surface (*18–20*). The relative intensities of the transitions to the $\frac{3}{2}$ and $\frac{1}{2}$ levels of the excited state designated by $I_{3/2}$ and $I_{1/2}$, respectively, are given by

$$I_{3/2}(\theta) = I_0\langle \exp - i(K \cdot X)\rangle^2(1 + \cos^2\theta) \tag{4}$$

$$I_{1/2}(\theta) = I_0\langle \exp - i(K \cdot X)\rangle^2(\tfrac{5}{3} + \cos^2\theta) \tag{5}$$

where K is the wave vector of the γ-ray, X is the displacement vector of the active atom, and θ is the angle between the principal axis of the electric field gradient tensor and the direction of observation.

The ratio of the intensities can be reduced by arranging a random orientation of particles because of the differing values of $1 + \cos^2\theta$ and $\frac{5}{3} + \cos^2\theta$ to

$$R = \frac{I_{3/2}}{I_{1/2}} = \frac{\int_0^1 (1 + u^2)\exp(-\epsilon u^2)\,du}{\int_0^1 (\frac{5}{3} - u^2)\exp(-\epsilon u^2)\,du} \tag{6}$$

where $u = \cos\theta$ and $\epsilon = K^2\langle Z^2\rangle - \langle X^2\rangle$. Here $\langle Z^2\rangle$ and $\langle X^2\rangle$ are the mean square amplitudes of the vibrations parallel and perpendicular, respectively, to the electric field gradient tensor. A measurement of the absolute Debye–Waller factor would give $\langle X^2\rangle$ and $\langle Z^2\rangle$ but this is difficult to make.

A later study (*21*) showed that the quadrupole splittings obtained from finely divided α-Fe_2O_3 particles absorbed on alumina and silica were identical. The absence of octahedral sites in silica rendered the earlier explanation inadequate and the new observation was interpreted in terms of the adsorption of identically small superparamagnetic ferric oxide particles. The importance of Mössbauer spectroscopy in subsequent investigations of the nature of this phenomenon has been the subject of a separate review (*22*). The six-line spectrum of bulk α-Fe_2O_3 arises from room-temperature weak antiferromagnetism. The magnetic ordering is a cooperative property and is volume and temperature dependent. When the microcrystallites are sufficiently small, thermal energy overcomes the cooperative forces aligning the magnetic moments of the ferric ions thereby allowing them to change rapidly from one direction to another as in paramagnetic compounds

to give an averaged zero effect during the time of measurement (*23–25*). When the relaxation time is shorter than the period for precession of the nuclear spin about the direction of the effective magnetic field, the substance is said to be superparamagnetic and the six-line Mössbauer spectrum collapses to two lines.

Subsequent work (*26*) by Kundig *et al.* used the changes in the peak areas that accompany the transition from the magnetically ordered to the superparamagnetic state to determine the crystallite sizes. A Larmor frequency for the ^{57}Fe nucleus in α-Fe_2O_3 was calculated (*26, 27*)to be 4×10^7 sec^{-1}, which corresponds to an observer relaxation time of 2.5×10^{-8} sec. The relaxation time, τ, for the spontaneous change in direction of the magnetic moment in single domain crystallites with uniaxial anisotropy may be written:

$$\tau = \frac{I}{f}\exp\left(\frac{Kv}{kT}\right) \tag{7}$$

where Kv is the energy barrier containing the magnetocrystalline anisotropy constant K and the volume v, T is the temperature, k is the Boltzmann constant, and f is set equal to the gyromagnetic precessional frequency of the magnetization vector about the effective field.

In a single-domain particle of α-Fe_2O_3 the magnetization vector is held in the c-plane perpendicular to the c-axis by the magnetocrystalline field. Mössbauer studies use the ^{57}Fe nucleus as the "observer" to record when the relaxation time τ becomes shorter than the period for precession of the nuclear spin about the direction of the effective field. Substitution into the equation for the Larmor frequency, or observer relaxation time, with an expression for the frequency factor proportional to the specific volume and anisotropy constant of the oxide gave (*26, 27*) the relationship:

$$\ln(2 \times 10^{-4}K) = \frac{Kv}{kT} \tag{8}$$

The value of K was obtained either from spectra of a series of samples having known average particle sizes at constant temperature or from spectra recorded as a function of temperature of a sample of known particle size. The determination of K was made at the point where half the total area under the spectrum resulted from the Zeeman pattern and the other half from the superparamagnetic fraction. Spectra used for such calculations are exemplified in Fig. 4. These spectra (*28*) were obtained from microcrystalline α-Fe_2O_3 produced by thermal decomposition of ferric nitrate on silica gel and subsequent

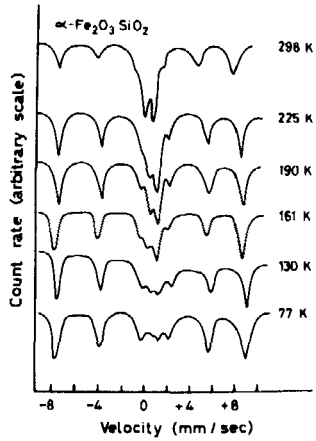

FIG. 4. Mössbauer spectra of α-Fe_2O_3 supported on silica gel as a function of temperature of the sample. [From M. C. Hobson and H. M. Gager, *J. Catal.* **16**, 254 (1970).]

calcination. Crystallite size measurements and the microcrystallite distribution was expressed in terms of mixtures of large antiferromagnetic and small superparamagnetic particles and were supported by X-ray diffraction data. The size and distribution was found to depend on the extent of calcination. Other results (*26*) showed that the quadrupole splitting increased from 0.44 mm sec^{-1} for microcrystals, which were reported to be of 180 Å diameter, to 0.57 mm sec^{-1} for crystals of 135 Å diameter. Smaller particles gave larger quadrupole splittings (0.98 mm sec^{-1}), whereas larger particles gave six-line spectra characteristic of magnetically ordered, bulk α-Fe_2O_3. The finely divided, supported α-Fe_2O_3 was not observed to undergo a Morin transition.

Further studies of this phenomenon (*29*) were reported as indicating that supported nickel oxide microcrystals doped with ^{57}Co on silica gel gave spectra consistent with the presence of ferric ions whereas the bulk material gave spectra corresponding to a mixture of both ferrous and ferric ions. An estimate of the nickel oxide particle size was made, and a later report (*30*) described the reduction of the nickel oxide to nickel of 60 Å diameter. Mössbauer studies of relaxation times and the transition to the superparamagnetic state with and without the presence of a magnetic field were described. It should be noted here that such source experiments are often complicated, and the consequences of nuclear transformations that involve both oxidation and reduction are not fully understood. Subsequent studies of small-particle relaxation times of Co_3O_4 on silica gel were reported

(*31*), and the calculation of microcrystallite size were supported by values obtained from X-ray line-broadening experiments.

The correlation of Mössbauer parameters with particle size involves the use of the "shell model" that describes the environment of surface nuclei as being of a lower symmetry than those within the particle. The model has been used to rationalize superimposed quadrupole-split spectra in terms of interior and surface iron nuclei.

The first of these reports (*27*) described the spectrum of a supported, iron oxide, microcrystallite sample as being composed of two superimposed doublets, the most prominent having a quadrupole splitting, Δ, of 1.38 mm sec^{-1}. The spectrum was attributed to the presence of different sized particles arising from lattice expansion or chemical modification of the surface shell. Similar conclusions were reported in the following year by Hobson from an independent study of the variation of quadrupole splitting with particle size (*32*). Other studies (*33*, *34*) suggested that the increase in quadrupole splitting with decreasing particle size was the result of homogeneous lattice expansion throughout the whole crystal lattice.

Application of the shell model to the study of catalysts implies that a decrease in particle size occurs with an increase in dispersion and that the resolution of separate quadrupole splittings for surface and bulk nuclei should be possible. It would appear important, when using this model, that consideration be given to the dependence of the quadrupole splitting for a highly dispersed system on the gaseous environment of the surface atoms (*35*) and also the lattice distortion of the particle due to internal pressure effects (*8*, *32*, *34*). It is also important that the factors giving rise to the quadrupole splittings are fully appreciated. Mössbauer studies of minerals (*36*) have clearly demonstrated the sensitivity of Mössbauer parameters to changes in the geometry of the ligand environment when the nearest ligands to iron remain the same. In the supported, iron oxide microcrystallites, as in many minerals, the immediate ligand to an iron atom is oxygen. It would, therefore, be expected that the Mössbauer parameters of supported, iron oxide microcrystallites would not only vary with oxidation state, electronic configuration, and coordination number, but also show marked dependence on the oxygen ligand environment. The Mössbauer investigations of minerals have demonstrated an overall correlation between the distortion of the oxygen octahedron and the quadrupole splittings. It has been shown that quadrupole splittings decrease with increased distortion according to the calculations (*37*) of the dependence of the quadrupole splittings in ferrous species on covalency effects and the distortion of the ligand environment from cubic symmetry.

An appreciation of these observations requires further consideration of the two major contributions to the quadrupole splitting which may be described as (*a*) the electric field gradient that arises from the electronic environment about the iron atom—the valence term; and (*b*) the electric field gradient originating from surrounding charged entities—the lattice term. The quadrupole splitting is proportional to V_{zz} the electric field gradient if both the valence and lattice charge distributions are considered as being symmetric about the *z*-axis:

$$V_{zz}/e = (I - R)q_{val} + (I - \gamma\alpha)q_{lat} \tag{9}$$

where q_{val} = valence contribution, q_{lat} = lattice contribution, and $(I - R)$ and $(I - \gamma\alpha)$ are Sternheimer antishielding factors.

Although these terms can in principle be calculated, their determination in practice is complicated by many factors (*37*). However, a cursory examination of small-particle iron oxide might well suggest that the interior iron nuclei would be expected to experience a reduced lattice contribution. The pure lattice contribution is, however, usually small and consequently any major modification and effect on the quadrupole splitting will only be observed if an appreciable number of iron nuclei occupy surface sites. Presumably the effect of microcrystallite size on the quadrupole splitting arises as a result of outer-layer ligand vacancies. It would seem to be inevitable that the electric field gradient at the superficial iron nuclei will be different from that at the nuclei in the bulk, and, consequently, it appears important that future investigations should concentrate on monolayers of supported iron oxide microcrystallites. Such investigations using samples enriched with ^{57}Fe, which would enhance the sensitivity of the Mössbauer technique, are feasible and the examination of 20 μg of ^{57}Fe, which occupies an area of 300 cm^2, should be possible.

Another method of correlating the superparamagnetic nature of ferric oxide with particle size has been described (*38–40*). It involves the computerized comparison of theoretically generated Mössbauer spectra for various relaxation times with the observed spectra of the highly dispersed systems.

The dependence of the isomer shift (*41*) and recoil-free fraction (*9*, *42–48*) on particle size has also been suggested, but such relationships may be somewhat tenuous. It is clear that caution must be exercised in the use of methods hitherto described in the interpretation and correlation of microcrystallite size. Recent work has suggested (*12*) that ferric oxide may react with the support when calcined at high temperatures, e.g. for 2 hr at 500°C. The presence and contribution

of such uncharacterized species to Mössbauer spectra of samples containing both large antiferromagnetic and small superparamagnetic particles renders the allocation of areas under specific peaks difficult, and it follows that the determination and interpretation of changes in peak areas that accompany the transition from the magnetically ordered state to the superparamagnetic state lack considerable precision. X-ray diffraction studies have failed to show the presence in these samples of any species other than α-Fe_2O_3, an observation suggesting that this physical method of characterization of solid surfaces may be unable, by itself, to establish the identity of all the important species on the surface. Subsequent studies of supported iron and iron oxide microcrystallites (*12*, *49*, *50*) and supported platinum and palladium iron clusters (*51–54*) have also indicated significant interaction between the metal and the support, illustrating that the inert supports are not as inert as they were once thought. Additionally, it is by no means clear that the size of particles that give Mössbauer parameters characteristic of surface nuclei are identical to those required for manifestation of the magnetic transitions used for making microcrystallite size determinations and that attempted correlations and interpretations must be prudently applied. Further, it is now appreciated how critically the quadrupole splitting depends on the chemical environment at the surface and that some supported microcrystallites at least are sensitive to the presence of atmospheric gases (*35*).

More recent studies of supported iron oxides have been directed toward an understanding of the nature of the adsorbed material. Table I illustrates the diversity of results that have been recorded for species giving quadrupole-split absorptions. Confusion still remains as to whether larger crystallites containing more defects tend to be found on silica gel or alumina (*55*, *56*). Some studies of the thermal decomposition of adsorbed iron salts on alumina, silica gel, magnesium oxide, chromium oxide, and zinc oxide have reported a higher dispersion of microcrystallites on alumina than on silica gel (*57*), and others (*49*) suggest that iron dispersion is influenced by both surface area and pore volume, both of which are reported to increase in silica gel samples with increasing iron concentration but to decrease in alumina samples. Some recent work has suggested that both europium (*58*) and ruthenium (*59*) form stronger interactions with alumina than with silica gel, and an iron oxide species that was initially uncharacterized (*28*) has subsequently been attributed to a reaction product with the support (*60*). Studies (*28*) of iron oxide samples reduced with hydrogen have shown that those supported on silica gel

TABLE I

IRON-57 MÖSSBAUER PARAMETERS FOR QUADRUPOLE-SPLIT SPECTRA OF SUPPORTED IRON OXIDE MICROCRYSTALLITES

Support	δ (mm sec^{-1})	δ(Fe) (mm sec^{-1})	Δ (mm sec^{-1})	Ref.
Alumina	0.45[a]	0.30	1.06	*17*
Silica	—	0.38	0.44	*26*
	—	0.32	0.57	*26*
	—	0.32	0.98	*26*
	—	—	1.38	*27*
	0.56[b]	0.31	0.69	*28*
	0.65[b]	0.40	0.74	*28*
	0.60[b]	0.35	0.77	*28*
	0.56[b]	0.31	0.71	*28*
	0.60[b]	0.35	1.17	*35*
	0.62[b]	0.37	0.84	*49*
	0.63[b]	0.38	0.73	*49*
α-Alumina	0.58[b]	0.33	0.71	*49*
	0.63[b]	0.38	0.72	*49*
η-Alumina	0.58[b]	0.33	0.95	*49*
	0.64[b]	0.39	0.82	*49*
γ-Alumina	0.59[b]	0.34	0.99	*49*
	0.60[b]	0.35	0.87	*49*
Alumina			0.97	*56*
	—	—	0.87	*56*
Silica			0.75	*56*
			1.82	*56*
	0.60[b]	0.35	0.75	*62*
	0.13[c]	0.31	0.60	*63*
	0.16[c]	0.34	0.75	*63*
	0.54[b]	0.29	1.87	*65*

[a] Values of δ relative to Fe/Cr.
[b] Values of δ relative to sodium nitroprusside.
[c] Values of δ relative to Co/Pd.

reproduced the original spectrum when reoxidized. Such behavior was not observed with the alumina-supported samples and was attributed to the reaction of iron in its reduced state with the support.

A six-line Mössbauer spectrum containing a superimposed doublet attributed to $ZnFe_2O_4$ was recorded (*50*) after $^{57}Fe_2O_3$ supported on zinc oxide was calcined at 400°C. The intensity of the doublet increased with higher calcining temperatures until, at 850°C, it was exclusive, demonstrating that reaction of Fe_2O_3 with the ZnO support had occurred. The controlled thermal degredation of ferricinium nitrate

(*61*) was reported to produce an iron oxide (mainly magnetite) in an inert carbonaceous matrix. The small particle size caused the material to be superparamagnetic down to and below 77 K, whereas at 4.2 K the material showed magnetic ordering with local disorder around the magnetic ions manifesting itself in a broadening of the spectrum.

Samples containing more than 10% by weight of supported iron oxide on alumina or silica have been shown to give a six-line Mössbauer spectrum corresponding to the antiferromagnetic character of large-particle ferric oxide (*56*, *62*). A group of Russian workers (*63*) investigated a sample of Fe_2O_3, prepared by the impregnation of silica gel with ferric nitrate, which gave a quadrupole-split Mössbauer spectrum similar to that previously reported (*64*) and which remained unchanged after outgassing at 500°C. The chemical isomer shift δ of 0.31 mm sec^{-1} was characteristic of a ferric species, and the quadrupole splitting Δ of 0.60 mm sec^{-1} was smaller than that reported elsewhere for small superparamagnetic Fe_2O_3 crystals, indicating a slightly larger crystallite size. The magnetic susceptibility, which was independent of the field strength, also suggested that the Fe_2O_3 particles were superparamagnetic. A similar two-line spectrum δ of 0.34 mm sec^{-1} was obtained from a sample prepared from $Fe(CO)_5$ in absolute ether, but the large quadrupole splitting of 0.75 mm sec^{-1}, a value also reported (*62*) for a sample containing 2% by weight of Fe_2O_3, suggested the presence of smaller particles. A third sample prepared from $FeCl_3$ gave a six-line spectrum corresponding to coarse α-Fe_2O_3 and possessed a magnetic susceptibility that varied with magnetic field strength. Many of the early Mössbauer spectroscopic studies of α-Fe_2O_3 microcrystallites supported on silica gel and alumina were repeated (*49*) in 1970 and the spectra classified according to whether they were six-line, two-line, or amalgams. For the two-line spectra, the chemical isomer shift, $\delta = 0.33$–0.37 mm sec^{-1}, fell within a narrow range characteristic of trivalent iron. The decrease in quadrupole splitting Δ from 0.99 to 0.71 mm sec^{-1} was attributed to variation in particle size from 40 to 130 Å. The transition from the superparamagnetic state to the antiferromagnetic state that occurred with increasing loadings of iron oxide was attributed to the increase in particle size.

Hobson and Campbell reported that the Mössbauer spectrum of a sample of iron oxide on silica gel, which has been calcined at 500°C for 16 hr, showed (*65*) a small chemical isomer shift of 0.29 mm sec^{-1} and an unusually large quadrupole splitting of 1.87 mm sec^{-1}. This splitting was noted to be larger than 1.60 mm sec^{-1} calculated by Flinn *et al.* (*17*) for a ferric ion in an octahedral environment with 1 oxygen atom missing but less than 2.26 mm sec^{-1} calculated for the

same model by using a more recent value of the Sternheimer antishielding factor (*66*). Both parameters were explained in terms of the presence of a very small particle, estimated by Kundig's methods (*26*) as being ca. 20 Å in diameter. The differences in chemical isomer shifts and quadrupole splittings produced by particles of different sizes were temperature-dependent and were tentatively associated with the number of defects in the crystal structure. Similar variations in Mössbauer parameters, although not so large, have been observed in ferric ions when located in octahedral and tetrahedral sites (*66*, *67*). The asymmetry of the two peaks was independent of temperature, unlike the initial (*17*) report, and the matter has recently been considered (*68*) and explained in terms of asymmetrical surface bonding producing a large electric field gradient, even though other workers have claimed a complete absence of asymmetry (*63*) when the crystallites are large.

It would be expected that the Goldanskii effect, which is the result of anisotropy of the recoil-free fraction in the γ-ray emission, would be observed in highly dispersed systems such as supported iron or iron oxide microcrystallites since the vibrational amplitude of the iron nucleus normal to the surface would not be likely to be the same as that parallel to the surface. If taken as being normal to the surface, V_{zz} would be expected to be large compared with the other two components and, consequently, the asymmetry parameter [Eq. (2)] would be small unless the difference between V_{xx} and V_{yy} was very large. Superimposed on this may be an asymmetry produced by relaxation effects (*65*). It has been shown (*69*) that for ferric ions the $\frac{1}{2} \rightarrow \frac{3}{2}$ transition begins to broaden before the $\frac{1}{2} \rightarrow \frac{1}{2}$ transition as the spin-lattice relaxation time of the 3d electrons approaches the Larmor precessional frequency of the nucleus when the temperature is lowered. The asymmetry thereby produced in the peaks is the reverse of the temperature dependence of the Goldanskii effect. It has been suggested (*65*) that temperature-independent asymmetry in supported microcrystalline materials may be interpreted in terms of the two effects being cooperative and canceling each other out over the temperature range concerned.

The linewidths of the Mössbauer spectra of supported iron oxide microcrystallites are larger than those recorded for iron in well-crystallized compounds and may suggest the superimposition of different quadrupole-split doublets arising from a number of ferric ions in a heterogeneity of sites.

It is possible that samples of alleged composition Fe_2O_3 may have been confused with hydrolyzed ferric species that give similar Mössbauer parameters (*70*, *71*). Authentic ferric oxide is known to give a

magnetically split, room temperature, Mössbauer spectrum when the particles are larger than 135 Å in diameter (*26*). Furthermore, it is reported (*72*) that only superparamagnetic particles smaller than 70 Å in diameter fail to show some magnetic hyperfine structure when cooled to 78 K. The species $Fe(OH)_3.0.9H_2O$ of ca. 39 Å diameter has been reported (*70*) to be superparamagnetic down to 10 K, and qualitatively similar spectra have been observed for samples with less water in the empirical formula, although their quadrupole splittings at 298 K were smaller, and magnetic hyperfine splitting at 4 K greater. The possibility that the particles might be γ-FeOOH, which is paramagnetic (*71*) at 77 K, cannot be ignored. It must also be remembered that the preparations of samples reported in the literature have varied considerably, and comparison of results must be made with caution.

B. Hydrogen Reduction of Iron Oxides

Initial studies (*55*, *64*, *73*) of the hydrogen reduction of supported Fe_2O_3 reported spectra, as depicted in Fig. 5, which were interpreted in terms of the superimposition of a ferrous doublet on a six-line metallic iron pattern. The reduction by hydrogen of large-particle Fe_2O_3, prepared by the impregnation of silica gel or alumina with an oxide loading in excess of 10% by weight, has been reported to give a surface mixture of ferrous oxide and metallic iron, whereas lower loadings were reduced to ferrous oxide only (*56*, *57*). The samples containing larger amounts of zero-valent iron were found to be more effective as catalysts for the hydrogenation of butene (*56*).

A somewhat contradictory study (*49*) reported that reduction at 450°C for 8 hr transformed magnetically ordered Fe_2O_3 to iron, whereas superparamagnetic specimens of supported Fe_2O_3 were reduced to metallic iron–ferrous iron mixtures. The degree of transformation of

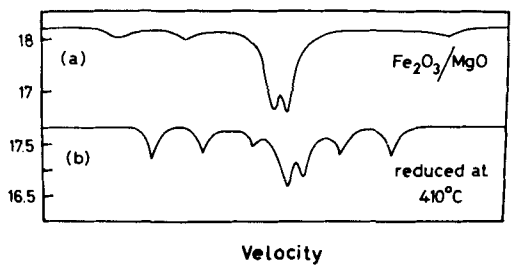

FIG. 5. Mössbauer spectra of supported Fe_2O_3 before and after reduction with hydrogen. [From H. Koelbel and B. Kuespert, *Z. Phys. Chem.* (*Frankfurt*) **69**, 313 (1970).]

the superparamagnetic state to the ferromagnetic state by heat treatment at 780°C for 16 hr showed good agreement with the degrees of reducibility. The metal-support interaction was reported to decrease in the order γ-alumina > silica > η-alumina > α-alumina, but the nature of the interaction was not investigated.

Hobson reported that the reduction of small-particle α-Fe_2O_3 on silica gel by hydrogen followed by evacuated heating at 450°C resulted in products that gave three-peaked Mössbauer spectra (*74*). A doublet, thought to represent a high-spin ferrous species, $\delta = 1.04$ mm sec^{-1} and $\Delta = 1.64$ mm sec^{-1}, containing a superimposed central peak, was distinguished and the composite spectrum attributed to the presence of iron atoms in two different states. The spectrum was interpreted in terms of a surface mixture of small-particle ferrous and ferric oxide, the second peak of the latter being superimposed on one of the peaks of the ferrous doublet. Other investigations have been performed, and the results are given in Table II.

Similar spectra have subsequently been reported (*65*) and are shown in Fig. 6. The variation in the intensities of the three peaks with temperature and length of reduction were interpreted in terms of the dependence of the Fe^{3+}/Fe^{2+} ratio on the conditions of hydrogen

TABLE II

IRON-57 MÖSSBAUER PARAMETERS FOR QUADRUPOLE-SPLIT SPECTRA OF SUPPORTED IRON OXIDE MICROCRYSTALLITES REDUCED IN HYDROGEN

Temperature (°C)	Peak	δ (mm sec^{-1})[a]	δ(Fe) (mm sec^{-1})	Δ (mm sec^{-1})	Ref.
200	1–2	1.02	0.77	0.98	*65*
	1–3	1.36	1.11	1.65	*65*
	2	1.51	1.26		*65*
300	1–2	1.04	0.79	0.99	*65*
	1–3	1.36	1.11	0.63	*65*
	2	1.54	1.29	-	*65*
450	1–2	1.07	0.82	1.01	*65*
	1–3	1.43	1.18	1.72	*65*
	2	1.58	1.33	—	*65*
450	1–3	1.29	1.04	1.64	*74*
	1–2	0.96	0.71	0.99	*74*
	2	1.46	1.21	—	*74*

[a] Values of δ relative to sodium nitroprusside.

reduction. Two surface iron sites were tentatively ascribed to a ferric ion, $\delta = 0.77$ mm sec^{-1} and $\Delta = 0.98$ mm sec^{-1}, and a high-spin ferrous ion, $\delta = 1.11$ mm sec^{-1} and $\Delta = 1.65$ mm sec^{-1}. These data were reinterpreted (*75*) in 1970 on the assumption that high-spin ferric ions in oxide environments normally have chemical isomer shifts of ca. 0.6 mm sec^{-1} and that the data could be interpreted in terms of a model (*76*) in which small surface cubo-octahedral crystals approximate spheres. Hobson and Gager (*75*) suggested that the samples were composed of microcrystalline ferrous oxide in which the ferrous ions occupied octahedral positions in a cubic lattice of oxide ions containing two distinct environments. The doublet characterized by the smaller chemical isomer shift and quadrupole splitting was attributed to a surface ferrous ion, i.e., a ferrous ion in an environment described by four oxide ions in the same plane and one below, whereas the other doublet was assigned to a ferrous ion within the interior of the deposit with six nearest oxide neighbors equally distributed above and below. The failure of the reduction process to go further than the ferrous state has been attributed to reaction of the adsorbed material with the support (*77*).

The quadrupole splitting for a ferrous high-spin compound arises from the valence, q_{val}, and lattice, q_{lat}, contributions to the electric field gradient. The q_{val} term has its origins in the field gradient resulting from the sixth d electron in ferrous compounds, but the total quadrupole splitting is smaller than the maximum value due to Boltzmann population of the upper d levels because of crystalline

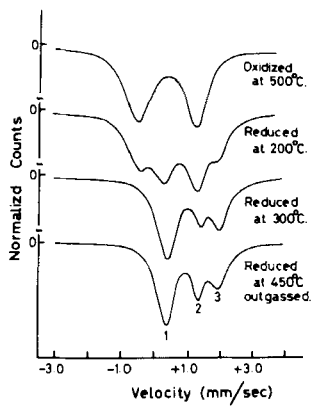

FIG. 6. Mössbauer spectra of 3% by weight iron on silica gel sample undergoing progressive reduction with hydrogen. [From M. C. Hobson and A. D. Campbell, *J. Catal.* **8**, 294 (1967).]

field and covalency effects that are difficult to calculate in complex systems. The lattice term, which originates from the surrounding charged entities, may be expressed as:

$$q_{\text{lat}} = \sum \frac{z_i \, 3 \cos_3{}^2 \theta_i - 1}{r_i} \tag{10}$$

where z_i is the charge on each atom, r_i is the distance of each atom from the iron nucleus, and θ_i is the angle that the atom subtends from the chosen z-axis.

Provided that the crystal structure is known, the q_{lat} term can, in principle, be calculated (*78*), although the correct assignment of charges to the different kinds of oxygen atoms in the structure and the convergence of the lattice term with increasing r and its sensitivity to small errors in crystallographic parameters are frequent sources of error. The prediction of quadrupole splitting by application of a ligand field method (*37*) that is independent of structural details has been shown to be successful in overcoming some of these difficulties. Although later results, obtained by a direct lattice summation technique (*79*), have contradicted some of the findings of the ligand field method (*37*), it does appear that a cautious application of the ligand field method may give useful information about surface structure. The method considers (*80, 81*) that a cubic ligand environment about iron in a ferrous compound gives little, or no, quadrupole splitting and that $q_{\text{val}} = q_{\text{lat}} = 0$. If, however, the ligand environment distorts slightly from cubic symmetry, then a very large (*82*) quadrupole splitting of ca. 3.70 mm sec^{-1} or higher may be observed and attributed almost exclusively to q_{val}. As the distortion of the ligand environment from cubic symmetry increases, the q_{lat} term increases and the quadrupole splitting decreases. It might, therefore, be expected that, in supported iron oxide microcrystallites, there would exist an overall correlation between distortion of the oxygen octahedra and the magnitude of the quadrupole splitting and which, in ferrous species, would result in smaller quadrupole splittings implying increased distortion.

C. Heating of Iron Oxides *in Vacuo*

The heating of a sample containing 2% by weight of α-Fe_2O_3 on silica gel at 475°C for 3 hr *in vacuo* (*62*) gave a product with Mössbauer parameters (see Table III) similar to those reported by Hobson *et al.* (*65, 74*) for the hydrogen-reduced specimens. Although one of the two superimposed doublets, $\delta = 0.80$ mm sec^{-1} and $\Delta = 1.14$ mm sec^{-1},

TABLE III

IRON-57 MÖSSBAUER PARAMETERS FOR QUADRUPOLE-SPLIT SPECTRA OF SUPPORTED IRON OXIDE MICROCRYSTALLITES HEATED IN VACUO

Temperature (°C)	Peak	δ (mm sec^{-1})[a]	δ(Fe) (mm sec^{-1})	Δ (mm sec^{-1})	Ref.
100	—	0.53	0.28	1.80	*35*
500	—	0.53	0.28	2.23	*35*
600	—	0.52	0.27	2.25	*35*
475	1–2	1.05	0.80	1.14	*62*
	1–3	1.37	1.12	1.77	*62*

[a] Values of δ relative to sodium nitroprusside.

was not identified, the authors concluded that heating *in vacuo* caused at least partial reduction to a ferrous species, as in the partial reduction of some powdered metal oxides, such as TiO_2 and MoO_3, by evacuated heating (*83*, *84*). Infrared spectroscopic evidence for the presence of ferrous ions in the surface of α-Fe_2O_3 that had been subjected to prolonged heating *in vacuo* (*85*) supports this hypothesis. The vacuum-reduced sample reproduced the original Mössbauer spectrum of supported α-Fe_2O_3 on silica gel after it had been exposed to oxygen at 1 atm pressure at 200°C. Reduction of the oxidized sample was reported to be impossible after threefold reduction and reoxidation, but reducibility was again achieved by exposing the sample to water vapor at room temperature. The water vapor appears to restore hydroxyl groups to the surface of the ferric oxide, and it is significant that such hydroxyl groups have been identified as likely active sites for surface chemical reactions on ferric oxide (*86*). Other investigations (*63*) have reported that coarse Fe_2O_3 samples heated at 500°C and at a residual pressure of 3×10^{-3} mm Hg give Mössbauer spectra consistent with partial reduction to ferromagnetic Fe_3O_4. These samples were found to have a greater magnetic susceptibility than the prereduced samples. These results (*62*, *63*) are contrary to those obtained by Gager *et al.* (*35*) who reported α-Fe_2O_3 supported on silica gel and calcined in air to give Mössbauer parameters of $\delta = 0.35$ mm sec^{-1} and $\Delta = 1.17$ mm sec^{-1}, which are consistent with high-spin ferric species (Fig. 7). When heated *in vacuo* at 100°, 500°, and 600°C, the quadrupole splitting increased to 2.25 mm sec^{-1}, a value that correlates well with Hobson's quadrupole splitting of 2.26 mm sec^{-1} calculated for an iron atom with one oxygen atom removed from its coordination sphere, and the chemical isomer shift decreased to 0.27 mm sec^{-1}. The exposure of the outgassed sample to dry oxygen produced no change in the Mössbauer spectrum implying

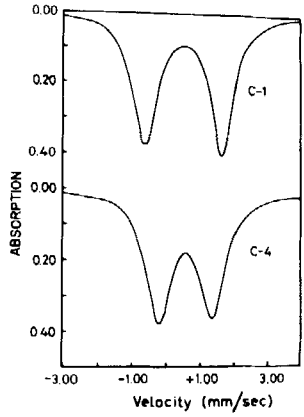

FIG. 7. Mössbauer spectra of α-Fe_2O_3. (C-1) Oxidized and outgassed at 600°C; (C-4) 205×10^{-3} mmole of water added. [From H. M. Gager, M. C. Hobson, and J. F. Lefelhocz, *Chem. Phys. Lett.* **15**, 124 (1972).]

physical, rather than chemical, adsorption of oxygen in accordance with the infrared evidence (*85*, *87*).

The reduction of microcrystalline iron oxide is clearly another area that requires further attention. Although α-Fe_2O_3 is reduced to iron metal at 673 K in hydrogen, it appears that the degree of reduction of supported iron oxide depends on particle size and the nature of the support and that, whereas antiferromagnetic large-particle α-Fe_2O_3 may be reduced to metallic iron, the paramagnetic or superparamagnetic phase is not. It may be possible at low surface concentrations for ferric ions to occupy sites in the surface that allow strong attraction between the iron and the support such that a complex similar to a surface silicate or aluminate would be formed. Reduction of this species to a ferrous complex may be possible, and it may be envisaged that such an entity would enable interior and superficial contributions to the Mössbauer spectra to be distinguished as has been achieved in the Mössbauer studies of minerals (*36*). Higher concentrations of ferric oxide may result in the iron atoms being less intimately bonded to the support, thereby making them less susceptible to its influence and more readily reducible to metallic iron. It is also possible that the superimposed doublet, which has frequently been observed, may be related to the iron oxide called wüstite (*88*), $Fe_{1-x}O$.

The principles involved in the investigations described in the foregoing may be important in future studies of the nature of catalysts. Weak interactions between a support and the catalytically active species may lead to sintering and a poorly dispersed catalyst, whereas

strong interaction may result in the stabilization of an undesired oxidation state of the catalyst. The nature of such interactions is amenable to investigation by Mössbauer spectroscopy if the catalytically active component contains a Mössbauer nucleus. In addition to the silica gel and alumina that have been discussed, carbon has been found to give too weak an interaction with iron (*89*) for catalytic usefulness, but magnesium oxide has demonstrated a potential utility for the preparation of highly dispersed metallic iron (*90*). It is still clear, however, that the synthesis of small, supported iron microcrystallites may necessitate the use of alternative methods of preparation. It is also clear that the support, although frequently considered as an inert carrier, may possess intrinsic activity due to surface acidity or through its interactions with small particles, and it is, therefore, not unreasonable to expect the support to be less inert as previously supposed.

Bartholemew and Boudart reported that the Mössbauer spectra of supported Pt—Fe clusters (*91*) permitted the resolution of both bulk and surface contributions to the spectra. The latter have been shown to be sensitive to the gaseous surface environment (*92*). Garten and Ollis (*93*) have investigated the particle size, composition, and component distribution in Fe—Pd clusters. The calculation of the size of metal atom clusters in which the atomic properties give way to the metallic properties (*51–53*) suggested that clusters of up to fifty atoms did not have the exact electronic structure of the bulk and that perturbation of the electronic structure of the metal particle by bonding with the support was probably significant. Such further evidence of support–crystallite interaction reinforces the previous cautionary comments on this matter and is again emphasized by some very recent work (*94*) comparing the chemical states of iron on silica gel and alumina with the chemical states of iron in platinum- or palladium-related catalysts. In spite of reports that ferric ions supported on SiO_2 or Al_2O_3 can only be reduced to ferrous ions at 500°C, the Mössbauer spectra show that reduction in the presence of platinum or palladium under similar conditions gives Pt—Fe and Pd—Fe clusters. The oxidation–reduction behavior of the iron and the spectral changes that occur on agglomerating the metals confirm this observation. It was shown that results obtained for the reduction of $PdFe/SiO_2$ catalysts at 700°C were different from those obtained for $PdFe/Al_2O_3$ catalysts and were attributed to the incorporation of silicon of the support into the PdFe clusters. Evidence for the formation of bimetallic clusters of PdFe and PtFe on Al_2O_3 and SiO_2 supports has also been reported and may be relevant to the recent application of supported bimetallic catalysts in refining petroleum.

D. Catalysts and the Adsorption of Gases

The application of the Mössbauer effect to the study of supported microcrystalline catalysts is currently receiving significant attention. Although the Mössbauer effect is primarily a solid-state bulk effect, the relatively high penetrating power of γ-radiation facilitates the investigation of catalytic pores, and, when a significant proportion of the Mössbauer nuclei are on the surface as supported microcrystallites, the active components of a catalyst may be readily investigated. The feasibility of monitoring the modification of the electric field gradient at the surface nuclei by Mössbauer spectroscopic investigation of monolayers of supported ^{57}Fe before and after the adsorption of gaseous molecules has been referred to earlier in this work. In principle, such investigations may be applied to the nature of the quadrupole splitting before and after use of the sample as a catalyst, while the sample is exposed to an adsorbing gas, or while the sample is actually operating as a catalyst.

Initial studies have involved the investigation of the effect on the Mössbauer spectrum of supported microcrystallites when exposed to polar molecules. Suzdalev *et al.* reported (*95*) microcrystalline ferric oxide to give a quadrupole-split Mössbauer spectrum characteristic of a ferrous species when carbon dioxide was adsorbed and the observation was attributed to the complex formation of a surface carbonate that could be reversed by heating *in vacuo*. Gager *et al.* (*35*) reported that α-Fe_2O_3 supported on silica gel that had been heated *in vacuo* at 600°C showed, when exposed to measured amounts of water vapor, a decrease in quadrupole splitting from 2.25 to 1.56 mm sec^{-1} and an increase in chemical isomer shift from 0.27 to 0.32 mm sec^{-1}. A subsequent report (*96*) gave parameters of $\delta = 0.35$ mm sec^{-1} and $\Delta = 1.17$ mm sec^{-1}. The quantitative addition of methanol and ammonia has also been shown to produce similar modifications of the Mössbauer spectrum (*35*), which were reversed by heating *in vacuo* and attributed to the hydration and subsequent dehydration at the surface. The dehydration process was presumed to decrease the number of nearest neighbors of the surface ferric ions thereby increasing the distortion of the electric field gradient to give an increased quadrupole splitting. Such changes in coordination number of surface cations following hydration and dehydration of oxides have been identified by other spectroscopic techniques (*97, 98*). Infrared spectroscopic evidence for the removal by outgassing of hydroxyl groups formed on activated α-Fe_2O_3 by the adsorption of water has also been reported (*83, 87*). The dependence of the quadrupole splitting on the chemical environment at the surface has been cited (*35*) as evidence for the inadequacy

of the shell (*27*) and lattice expansion (*33*, *34*) models for the determination of microcrystallite size. The attainment of reproducible and comparable results would require the calibration under some set of pretreatment conditions, such as rehydration to monolayer coverage. It must also be noted that aggregation by surface particles may result in a supported microcrystalline monolayer becoming multilayered.

Gager *et al.* (*96*) reported that treatment of an outgassed sample of supported α-Fe_2O_3 with hydrogen sulfide caused a decrease in the quadrupole splitting from 2.24 to 1.18 mm sec^{-1}. The chemical isomer shift, $\delta = 0.41$ mm sec^{-1}, confirmed that the iron remained in the ferric state. An additional Mössbauer absorption seen as a shoulder to the doublet at $\delta = 0.65$ mm sec^{-1} was regarded as an indication of either hydrogen sulfide occupying more than one type of adsorption site or the adsorption of a different species. Subsequent outgassing at room temperature failed to regenerate the original spectrum, indicating that chemisorption of hydrogen sulfide had occurred. Infrared spectroscopic data suggested that H_2S is dissociatively adsorbed to give HS^- and HO^- surface groups (*85*, *87*), and the additional peak in the Mössbauer spectrum was, therefore, attributed to one-half of a quadrupole doublet resulting from coordination of the HS surface group with the iron. The major doublet was considered to arise from the Fe—OH linkages, thereby giving a spectrum similar to that found with water.

Skalkina *et al.* (*99*) have considered the effect of adsorbed molecules on quadrupole splitting and have correlated values of Δ for iron in mixed oxides with catalytic activity for the ammoxidation of propylene.

Some work has also been attempted on the adsorption of polar molecules onto the surfaces of the reduced iron oxides. Chemisorption of ammonia was reported by Hobson (*74*) to produce a sample in which the extraneous center peak of the Mössbauer spectrum had disappeared (Fig. 8). It was suggested that amine radicals formed by chemisorption of ammonia transferred electrons to the adsorption site causing easy reduction of ferric to ferrous ions at the surface. The original spectrum was recovered by outgassing at elevated temperatures. Further work by Hobson and Gager (*75*) showed that the initial adsorption of ammonia had no effect on the spectrum of the reduced and outgassed sample, but that further addition of ammonia decreased the area of the relative center peak (attributed to half a doublet representing the surface ferrous species) of the three-peak spectrum. Heat treatment caused the desorption of ammonia until the original spectrum of the reduced and outgassed sample was recovered at 300°C. Complete desorption of the ammonia was not achieved, suggesting that the initial easy adsorption of ammonia was to the free hydroxyl

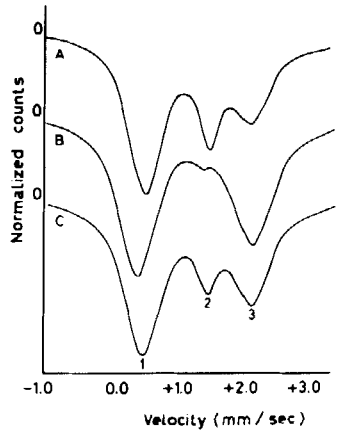

FIG. 8. Mössbauer spectra of adsorption and desorption of ammonia on an iron-on-silica gel catalyst at 25°C. [From M. C. Hobson, *Nature* (*London*) **214**, 79 (1967).]

groups of the silica [previously shown by infrared techniques to adsorb ammonia very strongly (*100*, *101*)] and the ammonia was shown to form a 1:1 surface complex with the surface ferrous ions. Another report by Hobson (*102*) showed that addition of ammonia to silica gel-supported iron caused a decrease in the quadrupole splitting of the outgassed ferric state and an increase in the surface ferrous state. The difference in behavior was explained by the factors that produce the electric field gradient. The five 3d electrons of a high-spin ferric ion are symmetrically distributed about the nucleus, and the ligands surrounding the ion are, therefore, primarily responsible for producing the electric field gradient. Addition of ammonia would be expected to increase the symmetry of the electric field gradient thereby decreasing the quadrupole splitting. The electric field gradient at the ferrous ion is a result of the lattice, the surrounding ligands, and also the extra 3d electrons. The last is reported to be usually quite large compared with the lattice and ligand contributions and to be of opposite sign (*37*). However, the sum of the contributions gives a relatively small quadrupole splitting for the surface ferrous ion, and, although the addition of ammonia increases the symmetry at the surface site, the net contribution to the electric field gradient of the ligands decreases. The sum of the 3d-electron and ligand contributions increases and, consequently, the quadrupole splitting increases.

Qualitatively the adsorption of methanol (*75*) gave a similar change in the Mössbauer spectrum to that observed for the adsorption of ammonia, but only half as much methanol was required to change the spectrum from its initial to final state. In accordance with the

infrared evidence (*100*), these observations were explained in terms of both strong chemisorption of methanol on the surface ferrous ion sites followed by dissociation and also by weak adsorption on the surface hydroxyl groups of the silica. Reaction on desorption to new products was also postulated. The adsorption of water vapor by the reduced and outgassed samples has also been investigated by Hobson *et al.* (*96*). The quadrupole splitting and chemical isomer shift were both found to increase to 1.90 and 1.07 mm sec^{-1}, respectively, which are parameters typical of high-spin ferrous iron. Outgassing at 500°C returned the spectrum to its original state.

The Mössbauer spectrum of ferrous Y-zeolite is somewhat similar to that of the reduced silica gel samples (*103*). The spectrum consists of two overlapping and partially resolved doublets with the inner doublet, $\delta = 0.89$ mm sec^{-1} and $\Delta = 0.62$ mm sec^{-1}, being attributed to the ferrous ion on the surface. In both the Y-zeolite and the reduced iron oxide on silica samples, the inner doublets representing surface ferrous states are the first to be affected by adsorption of polar molecules, but in the case of Y-zeolite the addition of excess amounts of water or ammonia causes the disappearance of the spectrum, and this has been interpreted in terms of "solvation" of the ferrous ions by absorbate causing weakening of the bonding to the crystalline lattice. It is also possible that the spectrum is a composite representing a multiplicity of parameters.

The spectral changes from three peaks to two were not observed when hydrogen sulfide was adsorbed on supported iron, although the quadrupole splitting did increase by 0.18 mm sec^{-1}. Pumping on the sample did not change the spectrum, suggesting that the H_2S is chemisorbed, and the difficulty in returning the sample to its original form was taken to indicate that either H_2S reacts directly with iron or, alternatively, dissociates on active sites of the silica gel and is followed by reaction of the resultant products with the iron surface sites to form iron sulfides. The latter explanation, supported by work on the adsorption of thiols on nickel (*104*) and Mössbauer studies of the reaction of H_2S with Raney iron (*105*) to give Fe_2S_3, was favored.

The use of Mössbauer spectroscopy to investigate the state of heterogeneous catalysts during catalysis (*106*) showed that when small particles of iron (ca. 5 nm) supported on magnesium oxide were used as catalysts for ammonia synthesis, the superparamagnetic portion of the spectrum was sensitive to both chemisorption of hydrogen and also to treatment of the particles by methods known to change their catalytic properties. It was suggested that surface iron atoms with seven nearest neighbors were particularly active for the ammonia synthesis.

A study of the oxidizing ammonolysis of propylene (*107*) by use of $Fe_2O_3 \cdot P_2O_5$ supported on silica gel showed that a small quadrupole splitting, corresponding to slight distortion of the lattice, gave CO_2, whereas samples with a larger quadrupole-split Mössbauer spectrum, indicating increased lattice distortion, were found to yield acrylic acid cyanide. It was suggested that catalytic selectivity and rate were determined by the degree of symmetry in the neighborhood of the iron. Another Mössbauer study (*108*) of mixed iron and antimony oxide catalysis for the ammoxidation of propene showed that Fe_2O_3 formed a compound with Sb_2O_5 or Sb_2O_3 when mixed with 25% by weight of SiO_2, which was believed to give $FeSbO_4$ as the active part of the catalyst. The isomer shift and quadrupole splitting for ^{57}Fe were correlated with the acrylonitrile yield, and a medium strength of lattice distortion or optimal change in the M—O bond was held responsible for a good selective oxidation catalyst. An electron-transfer mechanism was suggested as a necessity for activating the reacting molecules.

Accurate and reproducible Mössbauer spectra of supported iron catalysts require the prevention of the adsorption of impurities including oxygen and water onto the highly reactive sample surface. Cells designed to allow chemical reactions and *in vacuo* pretreatments at temperatures up to 673 K while the Mössbauer spectrum is being recorded have recently been reported and represent a significant and important development in the application of Mössbauer spectroscopy to catalytic and surface studies (*109–111*).

III. Tin

A limited number of Mössbauer studies of supported tin microcrystallites have been performed. Karasev *et al.* investigated (*112*) tetraphenyltin on silica gel under different conditions of temperature and pressure in an attempt to follow the nature of the adsorption process and to determine the structure of the adsorbed layers. Studies of chemisorbed tetraalkyltin on γ-Al_2O_3 reported the surface species to be SnR_4, $SnR_{4-n}(OMe)_n$ (n = 1,2,3), and $Sn(OMe)_4$, where OMe represents a surface oxygen–metal group (*113*, *114*). Investigations of the dynamic motion of tin atoms on silica gel have shown the presence of both tetravalent and divalent surface tin species (*115–120*). The temperature dependence of the intensity data has been interpreted in terms of physically adsorbed tetravalent tin and chemisorbed divalent tin (*115*). The electric field gradient at the ^{119}Sn nucleus in the adsorbed species increased with increasing temperature and was larger than that recorded for bulk crystalline SnO(*115*). The doublet peaks

for the adsorbed SnO showed considerable asymmetry (*115*) and a quantitative interpretation of the Goldanskii–Karyagin effect in tin was subsequently reported (*116*). Attempts to estimate the zero-point vibrations and the bond energies of the tin-support species (*112*) were subsequently shown to be of questionable significance (*121*). The dynamical properties of divalent tin ions and SnO_2nH_2O molecules adsorbed on silica gel have been reported to depend on the pore diameter of the silica gel (*117*). These studies on supported tin species (*115–120*) illustrate how recoil-free fraction and linewidth data obtained from the Mössbauer spectra may be used in the determination of the mobility of catalytic components. Such information is important because surface and bulk mobility frequently govern the degree of dispersion of the catalytically active phases.

Firsova *et al.* (*122*) reported that the room temperature Mössbauer spectrum of supported tin molybdate, which had been aged *in vacuo* at 723 K, showed the presence of tetravalent tin. Only after exposure to oxygen at 473 K did the sample act as an adsorbent for propylene. It then gave a Mössbauer spectrum that showed the reduction of the tetravalent tin to the divalent state. Reduction without exposure to oxygen was achieved at 673 K but supported tin in the absence of molybdenum was not reduced. The results were interpreted in terms of the proposals (*123*) for the synergistic oxidation–reduction during catalysis.

A recent *in situ* Mössbauer study (*124*) of a mixed tin–platinum oxide catalyst supported on zinc aluminate at 500°–600°C indicated the presence of tin(IV), tin(II), and an alloy of tin and platinum in the active catalyst. Changes in the nature of the tin species with time and temperature were correlated with the catalytic activity of the material.

IV. Gold, Europium, and Ruthenium

Mössbauer investigations (*125*) of magnesium oxide and alumina impregnated with solutions of $KAu(CN)_2$ and $HAuCl_4$ showed that thermal decomposition above 140°C occurred without complete decomposition to metallic gold. Mössbauer chemical isomer shift, electron diffraction, and X-ray broadening data indicated a distribution of gold crystals between 100 and 1000 Å. An uncharacterized electron-deficient gold species attributed to the interaction between the gold and the support was also identified.

Alumina, impregnated with $Eu(NO_3)_3$ solution and dried at 413 K, has been reported (*126*) to give a Mössbauer spectrum indicating the presence of a hydroxy oxide. Mössbauer studies (*127*) of the reduction

of trivalent europium supported on alumina showed that the fraction actually reduced was dependent on the europium-support interaction. This observation reinforces the findings of work involving supported iron microcrystallites and strongly suggests that the oxidation state of a supported catalyst depends on the interaction between the support and the active phase.

Mössbauer studies of the impregnation of silica with ruthenium chloride solution and subsequently dried at 383 K have reported (*59*) the presence of a ruthenium surface complex resembling $RuCl_3 \cdot xH_2O$. Recent work (*128*) has shown that Mössbauer spectra of ^{99}Ru supported on alumina, silica, activated charcoal, and X- and Y-zeolite are sensitive to the nature of the preparation and treatment of the samples.

Application of the Mössbauer effect, which is essentially a bulk phenomenon, to the study of surfaces has received significant attention in recent years. The usefulness of this technique lies in its ability to determine the electronic environment and symmetry of the surface nucleus, and it offers a method of investigation that is clearly complementary to other physical methods for the characterization of solid surfaces. Mössbauer spectroscopy has the attractive advantage that it may be used at a variety of pressures and can be applied to the study of heterogeneous catalysis and adsorption processes to probe the nature of the solid surface and its electronic modification when holding adsorbed species.

The first and most studied Mössbauer nucleus, iron-57, displays specific catalytic behavior. Mössbauer investigations of supported microcrystallites of iron and its oxide have demonstrated the importance of the techniques in the investigation of surface structure and chemistry. The application to other nuclei that have important catalytic qualities indicates the potential importance of the study of supported microcrystallites by Mössbauer spectroscopy in future investigations of catalysts. Developments in experimental techniques enabling *in situ* investigations are enhancing the scope of the technique.

ACKNOWLEDGMENTS

The author is indebted to Dr. A. G. Maddock for stimulating discussions during the writing of this work. The award of a Fellowship by I. C. I. Ltd. to the author is also acknowledged.

REFERENCES

1. Mössbauer, R. L., *Z. Phys.* **151**, 124 (1958).
2. Bancroft, G. M., Maddock, A. G., Ong, W. K., and Prince, R. H., *J. Chem. Soc.* p. 723 (1966).

3. Gibb, T. C., and Greenwood, N. N., *J. Chem. Soc.* p. 6989 (1966).
4. Epstein, L. M., *J. Chem. Phys.* **40**, 435 (1964).
5. Ablov, A. V., Belozerskii, G. N., Goldanskii, V. I., Makarov, E. F., Trukhtanov V. A., and Khrapov V. V., *Proc. Acad. Sci. USSR, Phys. Chem. Sect.* **151**, 712 (1963).
6. Lang, G., and Marshall, W. *Proc. Phys. Soc.* **87**, 3 (1966).
7. Herber, R. H., ed., *Am. Chem. Soc. Adv. Chem. Ser.* **68**, 30 (1966).
8. Schroeer, D., *in* "Mössbauer Effect Methodology" (I. J. Gruverman, ed.), Vol. 5, p. 141. Plenum, New York, 1969.
9. Goldanskii, V. I., and Suzdalev, I. P., *Russ. Chem. Rev.* **39**, 609 (1970).
10. Fluck, E., and Taube R., *in* "Development in Applied Spectroscopy" (E. L. Grove, ed.), Vol. 8, p. 244. Plenum, New York, 1970.
11. Hobson, M. C., *Progr. Surface Membrane Sci.* **5**, 1 (1972).
12. Hobson, M. C., *in* "Characterization of Solid Surfaces" (P. F. Kane, and G. B. Larrabee, eds.), p. 379. Plenum, New York, 1974.
13. Gager, H. M., and Hobson, M. C., *Catal. Rev.–Sci. Eng.* **11**, 117 (1975).
14. Delgass, W. N., *in* "Mössbauer Effect Methodology (I. J. Gruverman, and C. W. Seidel, eds.), Vol. 10. Plenum, New York, 1976.
15. Dumesic, J. A., *J. Phys. (Paris) Colloq. C6*, **37**, 279 (1976).
16. Kistner, O. C., and Sunyar, A. W., *Phys. Rev. Lett.* **4**, 412 (1960).
17. Flinn, P. A., Ruby, S. L., and Kehl, W. L., *Science* **143**, 1434 (1964).
18. Karyagin, S. V., *Dokl. Akad. Nauk SSSR* **148**, 1102 (1963).
19. Goldanskii, V. I., Gorodinskii, G. M., Karyagin, S. V., Korytko, L. A., Kriszhanski, L. M., Makarov, E. F., Suzdalev, I. P., and Khrapov, V. V., *Dokl. Akad. Nauk SSSR* **147**, 127 (1962).
20. Goldanskii, V. I., Makarov, E. F., and Khrapov, V. V., *Phys. Lett.* **3**, 344 (1963).
21. Constaboris, G., Lindquist, R. H., and Kundig, W., *Appl. Phys. Lett.* **7**, 59 (1965).
22. Collins, D. W., Dehn, J. T., and Malay, L. N., *in* "Mössbauer Effect Methodology" (I. J. Gruverman, ed.), Vol. 3, p. 103. Plenum, New York, 1967.
23. Neel, L., *C. R. Acad. Sci. Paris* **228**, 664 (1949).
24. Neel, L., *J. Phys. Soc. Jpn.* **17**, Suppl. B-1, 676 (1962).
25. Bean, C. P., and Livingston, J. D., *J. Appl. Phys.* **30**, 1205 (1959).
26. Kundig, W., Bömmel, H., Constaboris, G., and Lindquist, R. H., *Phys. Rev.* **142**, 327 (1966).
27. Kundig, W., Ando, K. J., Lindquist, R. H., and Constaboris, G., *Czech. J. Phys.* **17**, 467 (1967).
28. Hobson, M. C., and Gager, H. M., *J. Catal* **16**, 254 (1970).
29. Lindquist, R. H., Ando, K. J., Kundig, W., and Constaboris, G., *J. Phys. Chem. Solids* **28**, 2291 (1967).
30. Lindquist, R. H., Constaboris, G., Kundig, W., and Portis, A. M., *J. Appl. Phys.* **39**, 1001 (1968).
31. Constaboris, G., and Lindquist, R. H., *J. Phys. Chem. Solids* **30**, 819 (1969).
32. Hobson, M. C., *J. Electrochem. Soc.* **175c**, 115 (1968).
33. Schroeer, D., and Nininger, R. C., *Phys. Rev. Lett.* **19**, 632 (1967).
34. Schroeer, D., *Phys. Lett.* **27a**, 507 (1968).
35. Gager, H. M., Hobson, M. C., and Lefelhocz, J. F., *Chem. Phys. Lett.* **15**, 124 (1972).
36. Bancroft, G. M., Burns, R. G., and Maddock, A. G., *Geochim. Cosmochim. Acta* **31**, 2219 (1967).
37. Ingalls, R., *Phys. Rev.* **133**, A787 (1964).
38. Wickman, H. H., Klein, M. P., and Shirley, D. A., *Phys. Rev.* **152**, 345 (1966).
39. Blume, M., *Phys. Rev. Lett.* **18**, 305 (1967).
40. Blume, M., and Tjon, J. A., *Phys. Rev.* **165**, 446 (1968).

41. Schroeer, D., Marzke, R. F., Erickson, D. J., Marshall, S. W., and Wilenzick, R. M., *Phys. Rev. B* **2**, 4414 (1970).
42. Marshall, S. W., and Wilenzick, R. M., *Phys. Rev. Lett.* **16**, 219 (1966).
43. Suzdalev, I. P., Ya Gen, M., Goldanskii, V. I., and Makarov, E. F., *Soviet Phys. JETP* **51**, 118 (1966).
44. Akselrod, S., Pasternak, M., and Bukshpan, S., *Phys. Rev. B* **11**, 1040 (1975).
45. Roth, S., and Hörl, E. M., *Phys. Lett. A* **25**, 299 (1967).
46. Viegers, M. P. A., Van Eijkeran, J. C. H., Van Deventer, M. M., and Trooster, J. M., *Proc. Int. Conf. Mössbauer Spectrosc., 1975.*
47. Van Wieringer, J. S., *Phys. Lett. A* **26**, 370 (1968).
48. Ruppin, R., *Phys. Rev. B* **2**, 1229 (1970).
49. Yoshioka, T., Koezuka, J., and Ikoma, H., *J. Catal.* **16**, 264 (1970).
50. Winzer, A., Vogt, F., Schödel, R, Bremmer, H., and Wiesner, E., *Z. Chem.* **10**, 312 (1970).
51. Baetzold, A. C., and Mack, L. E., *J. Chem. Phys.* **6**, 1513 (1975).
52. Johnson, K., and Messmer, R. P., *J. Vac. Sci. Technol.* **11**, 236 (1974).
53. Fripiat J. G., Chow K. T., Boudart, M., Diamond, J. G., and Johnson, K. H., *J. Mol. Catal.* **1**, 59 (1975).
54. Garten, R. L. *in* "Mössbauer Effect Methodology" I. J. Gruverman, and C. W. Seidel, (eds.), Vol. 10. Plenum, New York, 1976.
55. Dunken, H., and Hobart, H., *Z. Chem.* **6**, 276 (1966).
56. Hobson, M. C., and Gager, H. M., *Proc. Int. Congr. Catal., 4th, 1968.* p. 28
57. Hobart, H., and Arnold, D., *Proc. Conf. Application Mössbauer Effect, 1969*, p. 325.
58. Ross, P. N., and Delgass, W. N., *J. Catal.* **33**, 219 (1974).
59. Clausen, C. A., and Good, M. C., *J. Catal.* **38**, 92 (1975).
60. See Hobson (*12*), p. 397.
61. Aharoni, S. M., and Litt, M. H., *J. Appl. Phys.* **42**, 352 (1971).
62. Tachibama, T., and Ohya, T., *Bull. Chem. Soc. Jpn.* **42**, 2180 (1969).
63. Rabashov, A. M., Fabrichnyi, P. B., Strakhov, B. V., and Babeshkin, A. M., *Russ. J. Phys. Chem.* **46**, 765 (1972).
64. Arnold, D., and Hobart, H., *Z. Chem.* **8**, 197 (1968).
65. Hobson, M. C., and Campbell, A. D., *J. Catal.* **8**, 294 (1967).
66. Nicholson, W. J., and Burns, G., *Phys. Rev.* **133**, A1568 (1964).
67. Armstrong, R. J., Morrish, A. H., and Sawatzky, G. A., *Phys. Lett.* **23**, 414 (1966).
68. Suzdalev, I. P., and Makarov, E. F., *Proc. Conf. Applications Mössbauer Effect, 1969*, p. 201.
69. Blume, M., *Phys. Rev. Lett.* **14**, 96 (1965).
70. Coey, J. M. D., and Readman, P. W., *Earth Planet Sc. Lett.* **21**, 45 (1973).
71. Johnson, C. E., *J. Phys. Chem.* [2] **2**, 1996 (1969).
72. Shinjo, T., *J. Phys. Soc. Jpn.* **21**, 917 (1966).
73. Koelbel, H., and Kuespert, B., *Z. Phys. Chem.* (*Frankfurt*) **69**, 313 (1970).
74. Hobson, M. C., *Nature* (*London*) **214**, 79 (1967).
75. Hobson, M. C., and Gager, H. M., *J. Colloid Interface Sci.* **34**, 357 (1970).
76. Van Hardeveld, R., and Hartog, F., *Surface Sci.* **15**, 189 (1969).
77. See Hobson (*12*), p. 390.
78. Burns, G., *Phys. Rev.* **124**, 524 (1961).
79. Nozik, A. J., and Kaplan, M., *Phys. Rev.* **159**, 273 (1967).
80. Shirane, G., Cox, D. E., Ruby, S. L., *Phys. Rev.* **125**, 1158 (1962).
81. Coston, C. J., Ingalls, R., and Drickamer, H. G., *Phys. Rev.* **145**, 409 (1966).
82. Johnson, C. E., Marshall, W., and Perlow, G. J., *Phys. Rev.* **126**, 1503 (1962).
83. Gebhardt, J., and Herrington, K., *J. Phys. Chem.* **63**, 120 (1958).

84. Ouchi, M., and Kusunoki, I., *J. Chem. Soc. Jpn.* **85**, 612 (1964).
85. Blyholder, G., and Richardson, E. A., *J. Phys. Chem.* **68**, 3882 (1964).
86. Okamoto, G., Furnichi, R., and Sato, N., *Electrochim. Acta* **12**, 1287 (1967).
87. Blyholder, G., and Richardson, E. A., *J. Phys. Chem.* **66**, 2597 (1962).
88. Greenwood, N. N., and Gibb, T. C., "Mössbauer Spectroscopy," p. 248. Chapman and Hall, London, 1971.
89. Kalvius, M., *in* "Mössbauer Effect Methodology" (I. J. Gruverman, ed.), Vol. 1, p. 163. Plenum, New York, 1965.
90. Boudart, M., Delbouille, A., Dumesic, J. A., Khammoma, S., and Topsoe, H., *J. Catal.* **37**, 486 (1975).
91. Bartholemew, C. H., and Boudart, M., *J. Catal.* **29**, 278 (1973).
92. Williams, I. L., and Nason, D., *Surface Sci.* **45**, 377 (1974).
93. Garten, R. L., and Ollis, D. F., *J. Catal.* **35**, 2 (1974).
94. Garten, R. L., "Mössbauer Effect Methodology" (I. J. Gruverman, and C. W. Seidel eds.), Vol. 10. Plenum, New York, 1976.
95. Suzdalev, I. P., Shkarin, A. V., and Zhabrova, G. M., *Kinet. Catal. USSR* **10**, 179 (1969).
96. Gager, H. M., Lefelhocz, J. F., and Hobson, M. C., *Chem. Phys. Lett.* **23**, 386 (1973).
97. Anderson, J. H., *J. Catal.* **28**, 76 (1973).
98. Dominique, P. H., and Danon, J., *Chem. Phys. Lett.* **13**, 365 (1972).
99. Skalkina, L. V., Suzdalev, I. P., Kolchin, I. K., and Margolis, L. Y., *Kinet. Katal.* **10**, 456 (1969).
100. Hair, M. C., and Hertl, W. J., *J. Phys. Chem.* **73**, 4269 (1969).
101. Folman, M., and Yates, D. J. C., *J. Phys. Chem.* **63**, 183 (1959).
102. See Hobson (*12*), p. 393.
103. Delgass, W. N., Garten, R. L., and Boudart, M., *J. Phys. Chem.* **73**, 2970 (1969).
104. Blyholder, G., and Bowen, D. O., *J. Phys. Chem.* **66**, 1288 (1972).
105. Arnold, D., Kuchnel, S., and Hobart, H., *Z. Anorg. Allg. Chem.* **379**, 35 (1970).
106. Dumesic, J. A., Maksimov, Y., and Suzdalev, I. P., *in* "Mössbauer Effect Methodology" (I. J. Gruverman, and C. W. Seidel, eds.), Vol. 10. Plenum, New York, 1976.
107. Shalkina, L. V., Suzdalev, I. P., Kolehim, I. K., and Ya Margolis, L., *Kinet. Catal.* **10**, 378 (1969).
108. Kriegsmann, H., Ohlmann, G., Scheve, J., and Ulrich, F. J., *Int. Congr. Catal. 6th 1976.*
109. See Dumesic, J. A., Maksimov, Y., and Suzdalev, I. P., *in* "Mössbauer Effect Methodology," (I. V. Gruverman and C. W. Seidel, eds.), Vol. 10. Plenum, New York, 1976.
110. Delgass, W. N., Chen, L. Y., and Vogel, G., *Rev. Sci. Instrum.* **47**, 136 (1976).
111. Dumesic, J. A., and Topsoe, A. H., *Adv. Catal.* **26**, 122 (1977).
112. Karasev, A. N., Polak, L. S., Shlikhter, E. B., and Shpinel, V. S., *Kinet. Katal.* **6**, 710 (1965).
113. Karasev, A. N., Polak, L. S., Shlikhter, E. B., and Shpinel, V. S., *Zh. Fiz. Khim.* **39**, 3117 (1965).
114. Karasev, A. N., Kolbanovskii, Yu. A., Polak, L. A., and Shlikhter, E. B., *Kinet. Katal.* **8**, 232 (1967).
115. Suzdalev, I. P., Goldanskii, V. I., Makarov, E. F., Plachinda, A. S., and Korytko, L. A., *Sov. Phys.—JETP* **22**, 979 (1966).
116. Suzdalev, I. P., Plachinda, A. S., and Makarov, E. F., *Sov. Phys.—JETP* **26**, 897 (1968).
117. Goldanskii, V. I., Neimark, I. E., Plachinda, A. S., and Suzdalev, I. P., *Teor. Eksp. Khim.* **6**, 347 (1970).

118. Goldanskii, V. I., Suzdalev, I. P., Plachinda, A. S., and Shtyrkov, L. G., *Dokl. Akad. Nauk SSSR* **169**, 872 (1966).
119. Suzdalev, I. P., Plachinda, A. S., Makarov, E. F., and Dolgopolov, V. A., *Russ. J. Phys. Chem.* **41**, 1522 (1967).
120. Kordynk, S. L., Lisichenko, V. I., and Suzdalev, I. P., *Kolloid Zh.* **33**, 374 (1971).
121. See Hobson (*12*), p. 389.
122. Firsova, A. A., Khovanskaya, N. N., Tsygranov, A. D., Suzdalev, I. P., and Margolis, L. Ya., *Kinet. Katal.* **12**, 792 (1971).
123. Margolis, L. Ya, *J. Catal.* **21**, 93 (1971).
124. Gray, P. R., *in* "Mössbauer Effect Methodology" (I. J. Gruverman, and C. W. Seidel, eds.), Vol. 10. Plenum, New York, 1976.
125. Delgass, W. N., Boudart, M., and Parravano, G., *J. Phys. Chem.* **72**, 3563 (1968).
126. Ross, P. N., and Delgass, W. N., *in* "Catalysis" (J. W. Hightower, ed.), Vol. 1, p. 597. North-Holland Publ., Amsterdam, 1973.
127. Ross, P. N., and Delgass, W. N., *J. Catal.* **33**, 219 (1974).
128. Clausen, C. A., and Good, M. C., "Mössbauer Effect Methodology," (I. V. Gruveman, and C. W. Seidel, eds.), Vol. 10. Plenum, New York, 1976.